

# In Situ Observation of Initial Rusting Process of Steel Containing Al Using Synchrotron Radiation X-Rays

J. Morimoto<sup>1,\*</sup>, M. Yamashita<sup>1</sup>, H. Uchida<sup>1</sup>, T. Doi<sup>2</sup>, T. Kamimura<sup>2</sup>,  
H. Miyuki<sup>2</sup>, H. Konishi<sup>3</sup>, and J. Mizuki<sup>3</sup>

<sup>1</sup>Graduate School of Engineering, University of Hyogo, Hyogo 671-2280, Japan

<sup>2</sup>Corporate Research and Development Laboratories Sumitomo Metal Industries, Ltd., Hyogo 660-0891, Japan

<sup>3</sup>Synchrotron Radiation Research Center, Japan Atomic Energy Agency, Hyogo 679-5148, Japan

We observed initial rusting process of steel containing Al under wet/dry cyclic condition with NaCl solution film using *in situ* X-ray diffraction spectroscopy at SPring-8 synchrotron radiation facility. It was found that mass fraction of iron oxides such as  $\alpha$ -FeOOH,  $\beta$ -FeOOH and  $\gamma$ -FeOOH varied with Al content. Some kinds of Al oxides were also found at the initial stage of corrosion. Those corrosion products might affect the corrosion process and corrosion rate of the steel.

**Keywords :** Steel; Rust; Al; Synchrotron radiation; X-ray diffraction

## 1. Introduction

Iron and steel are covered the rust layer consisting of some kinds of corrosion products as a result of atmospheric corrosion. Weathering steel containing small amount of Cr, Ni and Cu forms the protective rust layer during a long term exposure to the atmosphere. On the other hand, there exist some reports indicating that corrosion resistance of steel could be improved by adding Al as an alloying element.<sup>1),2)</sup>

In this study, *In situ* observation has been made for initial rusting process of steel containing Al under wet/dry cyclic condition with NaCl solution film using X-ray diffraction spectroscopy at SPring-8 synchrotron radiation facility.

## 2. Experimental method

### 2.1 Specimen

Specimen was a steel containing 1-8%Al with dimensions of 10 mm×10 mm×3 mm. The specimens were polished by series of emery papers until # 800, and were cleaned by alcohol between each step.

### 2.2 Corrosion chamber

Fig. 1 shows schematic illustration of the corrosion

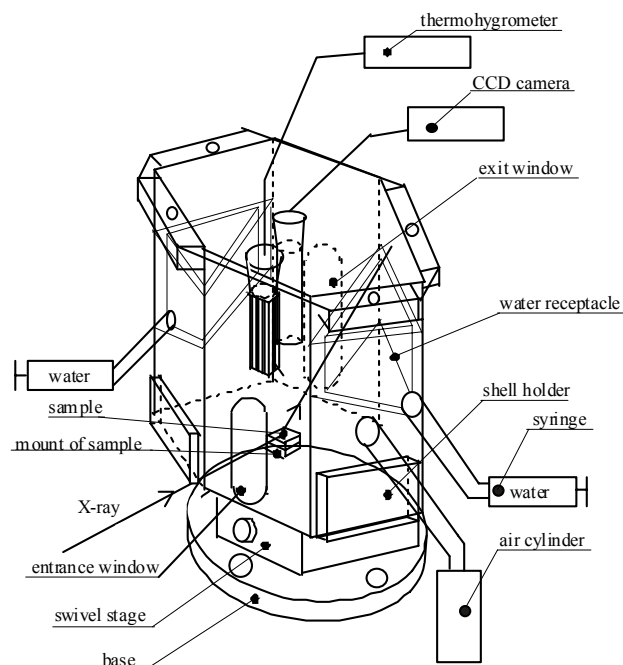


Fig. 1. Schematic illustration of corrosion chamber.

chamber. This chamber is made of transparent acrylic resin, so that the specimen on mount of sample inside the chamber can be seen. This corrosion chamber is fixed to swivel stage which can rotate the corrosion chamber from level and to the base made of stainless steel which is fixed on stage of X-ray diffraction machine.

\* Corresponding author: yamasita@eng.u-hyogo.ac.jp

The chamber has two water receptacles. Relative humidity inside the chamber can be controlled by water injection to and draining from the receptacles, and changing the dry air flow rate. The relative humidity and temperature were recorded by thermohygrometer. To reduce absorption of X-rays, X-ray windows are made of Kapton. To observe the corrosion process continuously, CCD camera is set up in the upper part of the chamber.

### 2.3 Experimental procedure

The specimen surface was covered with 100  $\mu\text{m}$  3.5%NaCl solution film which was obtained by pouring 1  $\mu\ell$  solution by hamilton syringe. X-ray diffraction measurement was continuously performed during the wet and dry stages. Each wet or dry cycle was performed every 125 min without interruption.

### 2.4 X-ray diffraction measurement

#### 2.4.1 *In Situ* energy dispersive X-ray diffraction

*In situ* observation was carried out using the energy dispersive X-ray diffraction (XRD) at BL14B1 in SPring-8 synchrotron radiation facility. This light source was originated from bending magnet. Because X-rays from the bending magnet was directly led to the experimental hatch without monochromator, we can obtain white X-rays. The incident angle and  $2\theta$  were fixed at  $1.0^\circ$  and  $3.5^\circ$ , respectively. Beam size molded in  $\sim 500 \mu\text{m} \times 50 \mu\text{m}$  by the slit.

#### 2.4.2 Angular dispersive X-ray diffraction

Synchrotron radiation X-rays at BL19B2 in SPring-8 was used. The powdered samples of corrosion products formed by the *in situ* wet/dry experiments have been dried more than 2 months in a desiccator, were firmly packed in a narrow Lindemann glass capillary (outer diameter 0.3 mm and glass thickness 0.01 mm) and positioned perpendicular to the X-ray beam with the linesegment shape sized 3.0 mm horizontal and 0.3 mm vertical. The wave length of X-ray was adjust to 0.075 nm that corresponds to 16.46 keV which avoided higher background signals due to fluorescence and was low enough to obtain satisfactory resolution. The diffraction intensity was recorded to an imaging plate.

## 3. Results and discussion

The XRD spectra of the rusts formed on the 1, 3, 5%Al-steels obtained by the *in situ* energy dispersive XRD observations are shown in Figs. 2-4. It is found from Fig. 2 that  $\text{Al}_2\text{O}_3$ ,  $\text{AlFeO}_3$ ,  $\text{Fe}(\text{OH})_3$ ,  $\gamma$ -FeOOH were formed at the initial stage of wet/dry cycling for the 1%Al-steel. Further wet/dry cycling resulted in the formation of  $\alpha$ -

FeOOH. For the 3%Al-steel,  $\text{AlFeO}_3$  was formed in the initial cycle as shown in Fig. 3, then  $\alpha$ -FeOOH,  $\beta$ -FeOOH,  $\gamma$ -FeOOH were formed. In addition,  $\text{Al}_2\text{O}_3$ ,  $\text{Al}(\text{OH})_3$  were also formed at the initial stage of the 5%Al-steel as shown in Fig. 4, but again ferric oxyhydroxides such as  $\alpha$ -FeOOH and  $\beta$ -FeOOH were formed in the subsequent stages.

Based on the *in situ* XRD results mentioned above, it can be pointed out that Al oxides and hydroxides initially formed and then ferric oxyhydroxides were grown; this implies that dissolved  $\text{Al}^{3+}$  is first forms Al compounds and, in the subsequent stages,  $\text{Al}^{3+}$  is enrolled in ferric oxyhydroxides.

The angular dispersive XRD results for the rust samples obtained by 2 months desiccation after the *in situ* wet/dry XRD experiments are shown in Fig. 5, where the result of Al-free carbon steel<sup>3)</sup> is also shown for reference. All the diffraction peaks from the rust can be assigned to ferric oxyhydroxides. Namely, no diffraction peaks due to Al compounds were found for the rust samples. This supports well the fact that Al is enrolled in ferric oxyhydroxides in the subsequent stages.

It is also noted that diffraction peak positions due to ferric oxyhydroxides shifted with increasing Al content, e.g. peaks at 0.270 nm and 0.419 nm due to  $\alpha$ -FeOOH shifted toward larger  $d$ -value with increasing Al content. So are the peaks due to  $\beta$ -FeOOH. This indicates that lattice spacing of ferric oxyhydroxides changes probably due to Al incorporation.

Fig. 6 indicates mass fraction of ferric oxyhydroxides in the rust samples estimated by the method<sup>4)</sup> developed by Hara *et al.* It can be said that the formation of  $\alpha$ -FeOOH was encouraged and/or crystal growth of  $\beta$ -FeOOH was suppressed with increasing Al content. This result is consistent with the report by Kamimura *et al.*<sup>5)</sup> who mentioned that  $\alpha$ -FeOOH increases with Al addition to steels exposed for 2 years Miyako-Island, Okinawa, Japan.

## 4. Conclusions

*In situ* observation of initial process of rust formation on the steel containing Al under wet/dry cycles with NaCl solution films has been discussed. Steel containing Al formed Al compounds such as  $\text{Al}_2\text{O}_3$  and  $\text{AlFeO}_3$  at the initial wet/dry stages and then, in the subsequent stages, ferric oxyhydroxides were grown. Some XRD peak positions of ferrous oxyhydroxides shifted toward larger  $d$ -value with increasing Al content, probably due to Al incorporation. It is also pointed out that the formation of  $\alpha$ -FeOOH was encouraged and/or crystal growth of  $\beta$ -FeOOH was suppressed with increasing Al content.

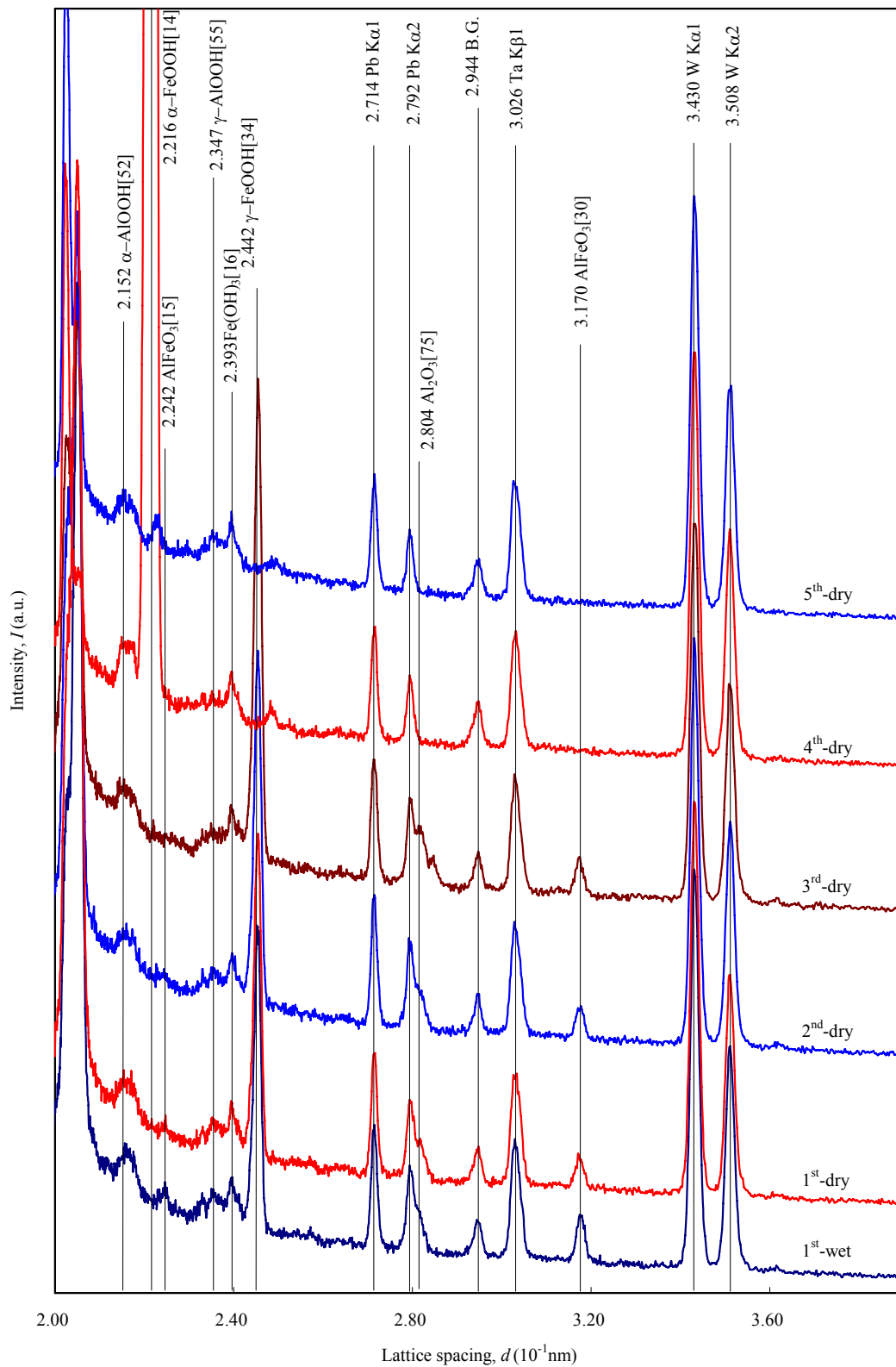


**Fig. 2.** *In situ* energy dispersive X-ray diffraction spectra of steel containing 1%Al covered with 3.5%NaCl solution film. Number in square bracket indicates the relative intensity in JCPDS data.

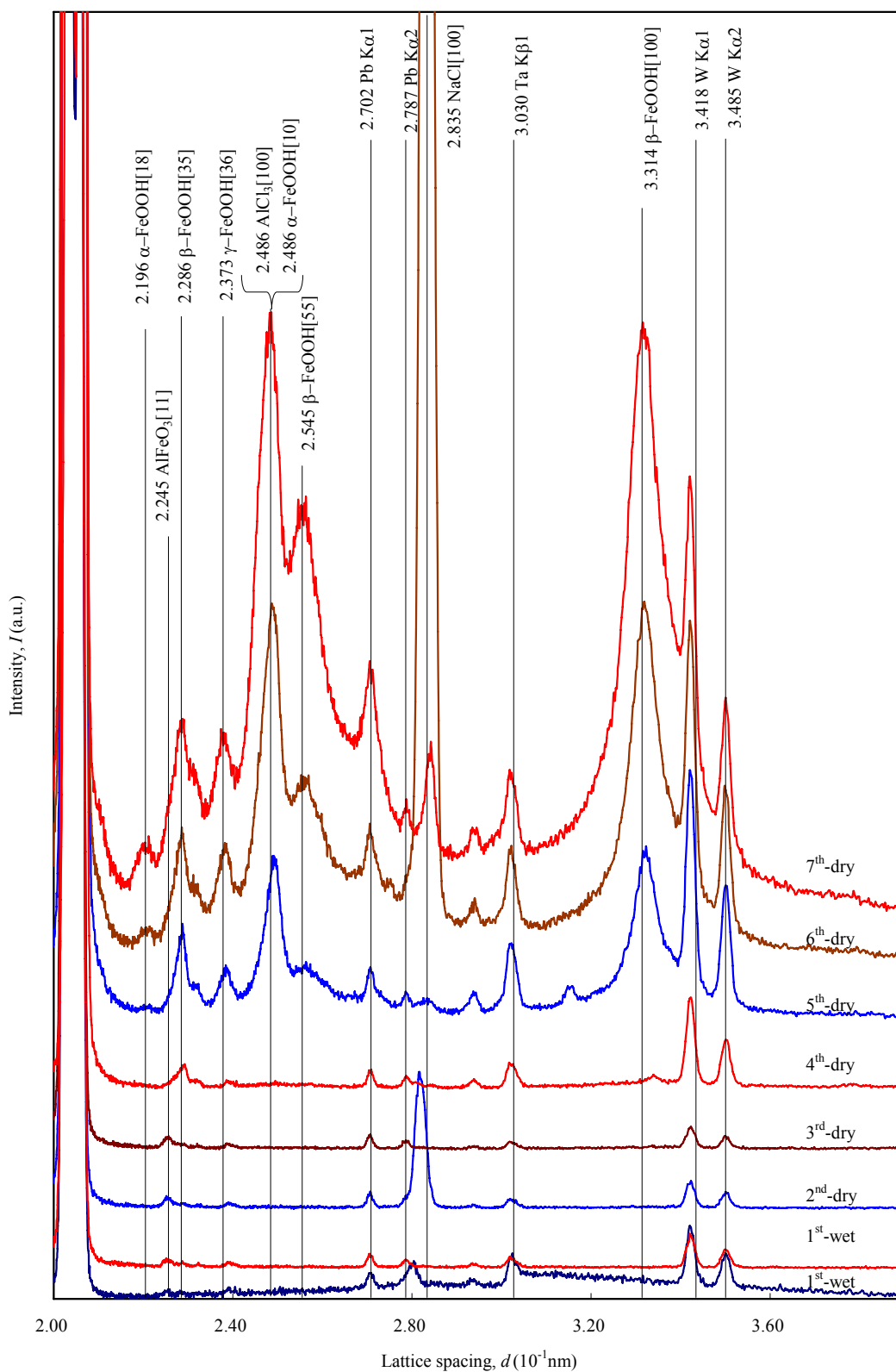


**Fig. 3.** *In situ* energy dispersive X-ray diffraction spectra of steel containing 3%Al covered with 3.5%NaCl solution film. Number in square bracket indicates the relative intensity in JCPDS data.

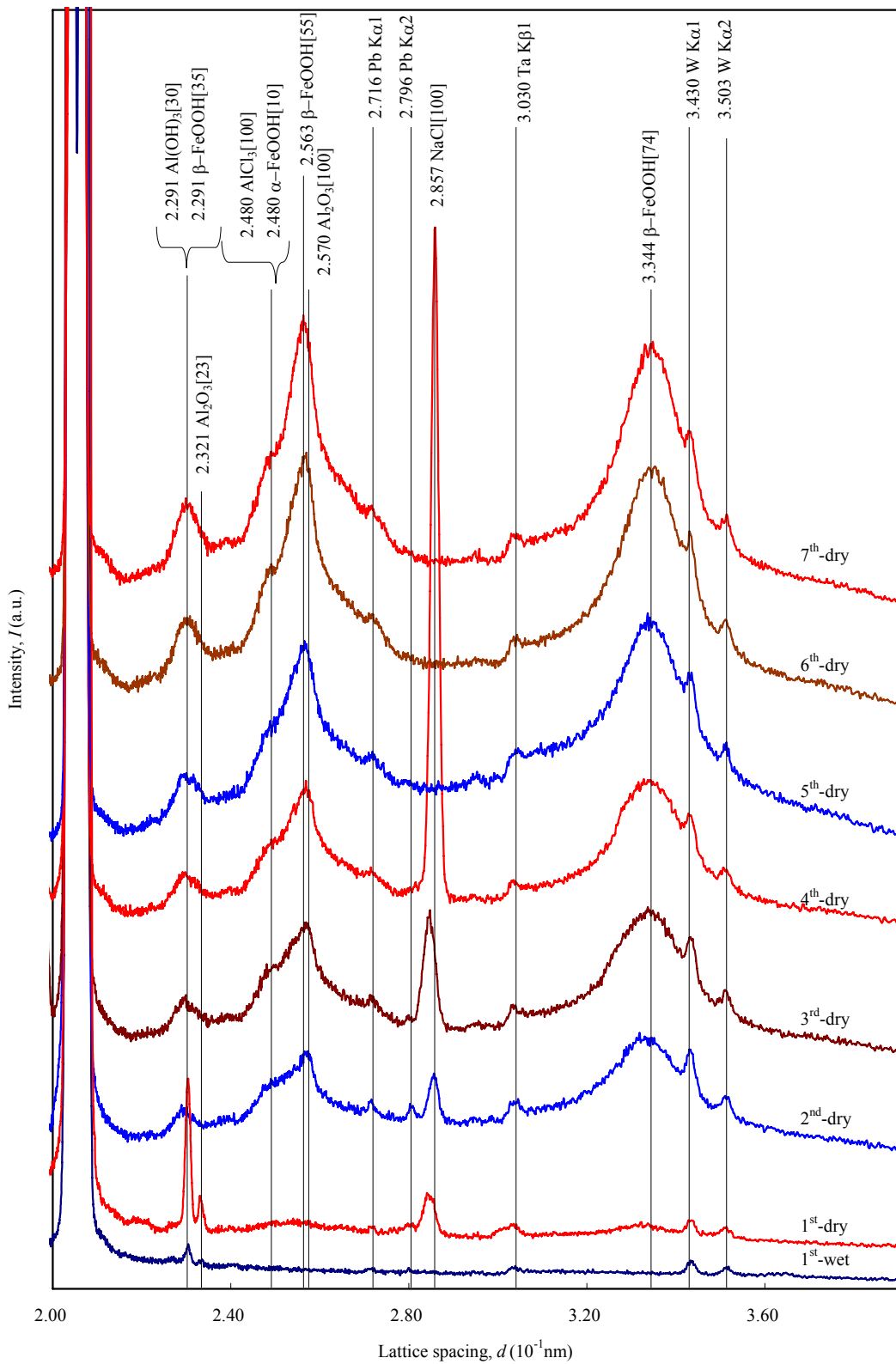


**Fig. 4.** *In situ* energy dispersive X-ray diffraction spectra of steel containing 5%Al covered with 3.5%NaCl solution film. Number in square bracket indicates the relative intensity in JCPDS data.

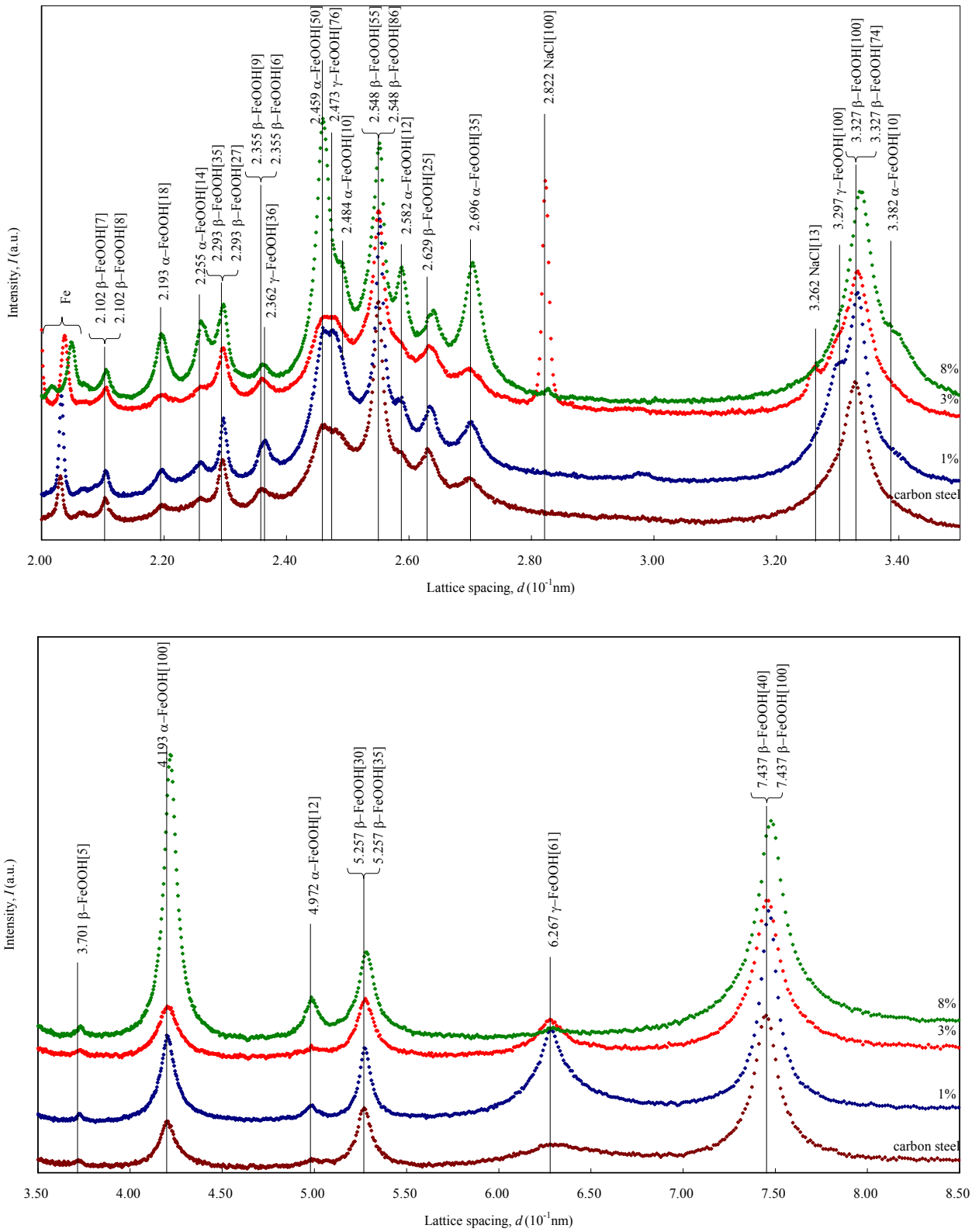


**Fig. 5.** Angular dispersive X-ray diffraction spectra of steel containing Al and carbon steel covered with 3.5%NaCl solution film. Number in square bracket indicates the relative intensity in JCPDS data.

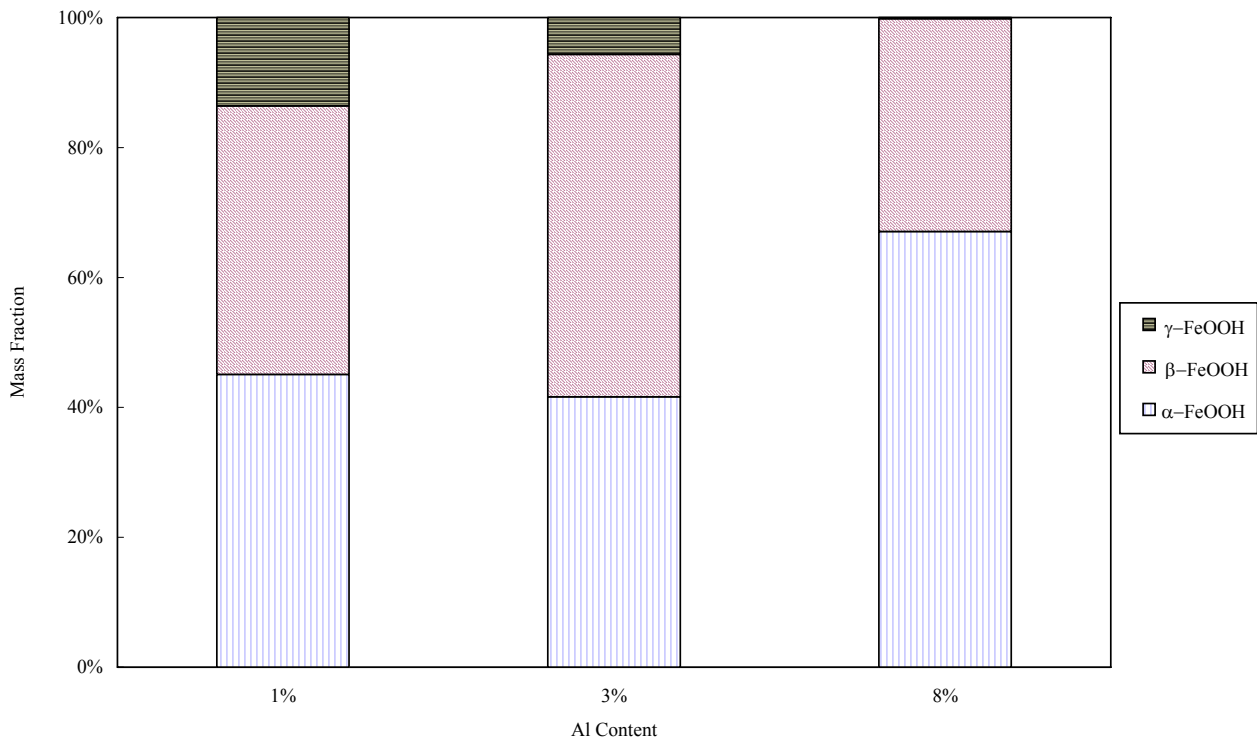


Fig. 6. Mass fraction of ferric oxyhydroxides in the rust samples.

### References

1. T. Nishimura, A. Tahara and T. Kodama, *J. Japan Inst. Metals*, **64**, 699 (2000).
2. N. Wagure, K. Kashima, T. Kamimura and H. Miyuki, *Proceedings of the 51st Japan Conference on Materials and Environments*, p.175 (2004).
3. M. Yamashita, H. Konishi, T. Kozakura, J. Mizuki, and H. Uchida, *Corrosion Science*, **47**, 2492 (2005).
4. S. Hara, M. Yamashita, T. Kamimura, M. Sato, *J. Japan Inst. Metals*, (2007) in press.
5. T. Kamimura, N. Wagure, K. Kashima, T. Doi, H. Miyuki, S. Nasu and S. Morimoto, *CAMP-ISIJ*, **18**, 1675 (2005).